Performance analysis of non-line-of-sight ultraviolet communication through turbulence channel

Tao Liu (刘 涛), Peng Wang (王 鹏), and Hongming Zhang (张洪明)*

State Key Laboratory on Integrated Optoelectronics, Tsinghua National Laboratory for Information Science and Technology; Department of Electronic Engineering, Tsinghua University, Beijing 100084, China

**Corresponding author: zhhm@tsinghua.edu.cn*

Received November 17, 2014; accepted January 28, 2015; posted online March 25, 2015

The bit error rate performance of non-line-of-sight ultraviolet communication through atmospheric turbulence is studied. The communication performance degradation under different strengths of turbulence is evaluated. Particularly, under strong turbulence conditions, the communication distance can be shortened by 30%, or at a given distance the communication rate can be reduced by half than the counterpart of no turbulence.

OCIS codes: 060.2605, 060.4510.

doi: 10.3788/COL201513.040601.

Free space optical communication, with wavelengths ranging from the infrared to UV has attracted considerable attention[1–3]. Compared with wireless communication, the advantages of optical communication lies in the huge unlicensed spectrum, low-power, miniaturized transceivers, and high security[4,5]. The motivation for using UV technology lies in: first, atmospheric scattering of UV radiation by molecules and aerosols provides a mechanism for establishing a non-line-of-sight (NLOS) communication link[6–9]. The NLOS link characteristic relaxed the acquisition, tracking, and pointing (ATP) requirement, greatly reducing the complexity of the communication system. Second, the strong ozone absorption of UV radiation in the upper atmosphere making the solar noise in the UV band is very low. In the end, recent development in UV transmitters and UV photomultiplier tube (PMT) detectors, and emerging requirements from the military and other applications have led to increasing interest in NLOS UV communication.

In the late 2000s, a series of experiments and theoretical analysis about LED-based NLOS UV communication were conducted[10–12]. However, these studies were confined to short range communication (below 100 m), and greatly limited its practical application.

To increase the communication distance, high-power UV-LED modules are used to increase the transmitter power. In the mean time, a high sensitivity PMT and wide field-of-view (FOV) receiver are used to improve the signal-to-noise ratio (SNR). In UV NLOS communication, on-off-keying (OOK) and pulse position modulation (PPM) are two commonly used modulation methods. Although OOK modulation and demodulation is relatively simple, PPMs have better flexibility and performance[12]. In our research 4-PPM is used as the modulation method.

For short range NLOS communication, the impact of atmospheric turbulence is ignored. As the range increases to hundreds of meters, the impact of turbulence on the performance of NLOS communication must be considered. In this Letter, the performance degradation of long range NLOS UV communication through a turbulence channel is studied, the bit error rate (BERs) are calculated and checked by Monte-Carol simulation under different baseline distances, different bit rates and different transmitter/receiver. The results and conclusions acquired in this Letter can be used to predict the achievable communication performance as a function of system and atmospheric parameters, and serve as the basis for the system design.

A typical single-scattered NLOS communication schematic diagram is illustrated[6], as shown in Fig. 1. The beam full-width divergence angle of the transmitter (T_x) is denoted by ϕ_1 and the FOV angle of the receiver (R_x) is denoted by ϕ_2. The T_x and R_x pitch angles are denoted by θ_1 and θ_2, respectively. The baseline distance is denoted by r and the distances of the intersected volume V to the T_x and R_x are denoted by r_1 and r_2, respectively.

From the communication point of view, scattering and absorption are two kinds of dominant interactions between photons and the atmosphere. Under the homogeneous atmosphere assumption, the total scattering by molecules and aerosols is defined as $k_s = k_s^{\text{ray}} + k_s^{\text{mie}}$, where k_s^{ray} and k_s^{mie} are Rayleigh and Mie scattering coefficients, respectively. The extinction coefficient is defined as $k_e = k_s + k_a$, where k_a is the absorption coefficient. The

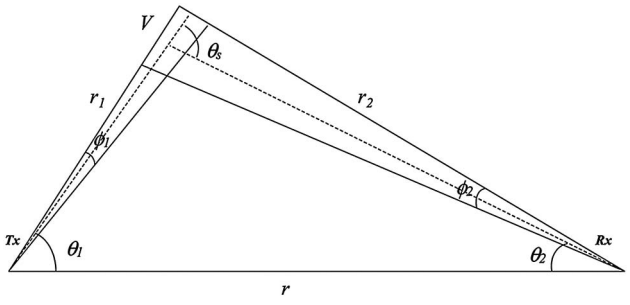

Fig. 1. Typical NLOS UV communication schematic diagram.

scattering phase function is modeled as a combination of the generalized Rayleigh function and generalized Henyey–Greenstein function, as suggested by[13]

$$p(\mu) = \frac{k_s^{\text{ray}}}{k_s} p^{\text{ray}}(\mu) + \frac{k_s^{\text{mie}}}{k_s} p^{\text{mie}}(\mu),$$
$$p^{\text{ray}}(\mu) = \frac{3[1+3\gamma+(1-\gamma)\mu^2]}{16\pi(1+\gamma)},$$
$$p^{\text{mie}}(\mu) = \frac{1-g^2}{4\pi}\left[\frac{1}{(1+g^2-2g\mu)^{3/2}} + f\frac{0.5(3\mu^2-1)}{(1+g^2)^{3/2}}\right], \quad (1)$$

where $\mu = \cos\theta_s$, θ_s is the scattering angle; γ, g, and f are function parameters.

A single-scatter model to calculate the pass loss of NLOS links was proposed[14]. While this model typically requires complex numerical calculations, a simplified approximate closed-form expression for pass loss is given by[15]

$$P_L \approx \frac{96r\,\sin\theta_1 \sin^2\theta_2 \left(1-\cos\frac{\phi_1}{2}\right)\exp\left[\frac{k_e r(\sin\theta_1+\sin\theta_2)}{\sin\theta_s}\right]}{k_s p(\mu) A_r \phi_1^2 \phi_2\,\sin\theta_s(12\sin^2\theta_2+\phi_2^2\sin^2\theta_1)}. \quad (2)$$

When the communication distance increases to hundreds of meters, the impact of atmospheric turbulence on the NLOS links becomes significant[16]. Atmospheric turbulence is caused by the random fluctuation of the atmospheric refractive index along the transmission path. This fluctuation is caused by random variations of atmospheric temperature from point to point[17]. The atmospheric turbulence will lead to the intensity fluctuation of the beam traversing the turbulent medium. The strength of the intensity fluctuation is given by[18]

$$\sigma_l^2 = 1.23 C_n^2 K^{7/6} L^{11/6}, \quad (3)$$

where C_n^2 is the refractive index structure constant, (which is used for characterizing the strength of turbulence), $K = 2\pi/\lambda$ is the wavenumber, and L is the link range. This equation is valid for $l_0 \le \sqrt{\lambda L} \le L_0$, where l_0 is the inner scale of turbulence and L_0; is the outer scale of turbulence.

Assuming that the log intensity l of the beam traversing the turbulent atmosphere is normally distributed. The probability density function (PDF) of the beam intensity $I = I_0\exp(l)$ is log normal distributed, given by[18]

$$p(I) = \frac{1}{I\sqrt{2\pi}\sigma_l}\exp\left\{-\frac{(\ln(I/I_0)+\sigma_l^2/2)^2}{2\sigma_l^2}\right\} \qquad I \ge 0, \quad (4)$$

where I_0 is the received intensity without turbulence.

We have to note that the log normal model is valid for turbulence with small values of σ_l^2; for $\sigma_l^2 \ge 1.2$, this model no longer holds[18]. More details of atmospheric turbulence can be found in Ref. [18].

The above analysis is the traditional line-of-sight (LOS) turbulence theory. In Ref. [19], a turbulence model of a NLOS UV link is provided based on the existing LOS turbulence theory applied to two LOS links: form transmitter to the common volume, and common volume to the receiver. Recently, based on the model of Ref. [19], a more accurate turbulence model is proposed[16]. In this model turbulence-induced scintillation attenuation is added and noncoplanar geometries are considered. Our turbulence model to evaluate the NLOS communication performance is also based on the model of Ref. [19], where the two-LOS link is treated as independent links. Since in each LOS link log-normal turbulence is assumed, the received irradiance distribution is also log-normal, and an analytical expression is achieved. While in the model of Refs. [16, 19], the received irradiance distribution is achieved by numerical integration.

In Ref. [16], the receiver noise model is treated as additive white Gaussian noise (AWGN), and the communication performance of OOK modulation under turbulence condition is evaluated. In our paper, the receiver noise is treated as a mixed noise model, which is the combination of Gauss noise and Poisson shot noise. This noise model is relatively more accurate than the AWGN. The communication performance of PPM is evaluated.

Because of the severe attenuation of a UV beam in the NLOS propagation channel, it usually calls for a PMT to receive the weak signals. The PMT have high amplification factors and low dark counts, especially suitable for long range communication. The decision variable is expressed as $z = s + n$, where s is the output current of the PMT and n is the thermal noise produced by the postprocessing circuit.

The thermal noise is modeled as a zero mean Gaussian random variable with variance given by[20]

$$\sigma_n^2 = \left(\frac{2k_e T}{R_L T_p}\right), \quad (5)$$

where k_e, T, R_L, and T_p denote the Boltzmann constant, receiver temperature, load resistance, and the pulse interval of the PPM.

The arrival of primary photoelectrons obey the Poisson distribution, with a mean λ given by

$$P_{k1}(j|\lambda) = \frac{\lambda^j}{j!}e^{-\lambda}, \quad (6)$$

The multiplication gain of the PMT for each primary photoelectron is denoted by $\{g_i\}$ and is supposed to be an independent and identical Gaussian random variable[21]; the output current of the PMT is represented as

$$s = \sum_{i=1}^{k1} g_i e, \quad (7)$$

where e is the electron charge. The conditional PDF of z can be written as[12]

$$P_z(z|\lambda) = \sum_{j=0}^{\infty} P_{k1}(j|\lambda)\, G(z, jge, \sigma^2),$$

$$\sigma^2 = \sigma_n^2 + \sigma_{\mathrm{PMT}}^2 = \left(\frac{2k_e T^0}{R_L T_p}\right) + j(\zeta g e)^2, \qquad (8)$$

where $G(a, b, c)$ denotes a Gaussian PDF of variable a with mean b and variance c. g is the average gain of the PMT; the variance σ^2 is the combination of the thermal noise variance and random gain effect of the PMT, and ζ is the PMT spreading factor.

PPM is a pulse based modulation method where the receiver detects the signal by determining the optical energy in each possible time interval, then selects the signal with the maximum energy. The probability of the correct detection of the M-PPM symbol is given by[21]

$$P_D = \frac{1}{2^{M-1}} \sum_{j=0}^{\infty} \frac{(K_s + K_b)^j}{j!}\, e^{-(K_s+K_b)} \int_{-\infty}^{\infty} G(z, jge, \sigma^2) \times \left\{1 + \sum_{k=0}^{\infty} \frac{{K_b}^{k_e - k_b}}{k!}\, \mathrm{erf}\left(\frac{z - kge}{\sqrt{2}\sigma}\right)\right\}^{M-1} \mathrm{d}z, \qquad (9)$$

where $\mathrm{erf}(x)$ is the error function, $K_b = N_n T_p$ is the average background photon count per pulse; it is the product of pulse duration time T_p and background noise count rate N_n, which is acquired by experiment[7]. $K_s = \eta M P_t T_p/(P_L h\nu)$ is the average signal photon count per pulse. η, h, ν, P_t, and P_L denote the overall quantum efficiency of the optical filter and photodetector, Planck's constant, the frequency of the UV optical, and the average transmitted power and path loss, respectively. The BER of M-PPM can be derived from P_D and written as[4]

$$P_{e\_\mathrm{PPM}} = 0.5M/(M-1)(1 - P_D). \qquad (10)$$

Under turbulence conditions, the received optical intensity $I = K_s(h\nu)$ is no longer a constant, and obeys a log-normal distribution, which means that it is the fluctuation of K_s that will causes the performance degradation of the NLOS communication. Assuming the perfect channel state information (CSI) is known, the mean BER of M-PPM can be numerically calculated by

$$\bar{P}_e = \int_0^{\infty} P_{e\_\mathrm{PPM}} p(I) \mathrm{d}I. \qquad (11)$$

To evaluate the impact of atmospheric turbulence on the performance of NLOS UV communication, a variety of numerical calculations and simulations are done under different strengths of atmospheric turbulence. A high-sensitivity PMT and a high-impedance amplifier are used to maintain a high SNR. The BERs under different baseline distances, different bit rates, and different T_x/R_x angles are calculated. The beam divergence of the transmitter and the FOV of the receiver are fixed. The typical system parameters and atmospheric parameters that are used for numerical calculation are listed in Table 1.

Table 1. Typical UV Communication Parameters

Parameter	Value
Signal wave length	250 nm
Transmitter average power P_t	1 w
Beam divergence of the T_x	60°
FOV of the receiver R_x	15°
Background noise count rate N_n	14,500 s^{-1}
Optical filter transmission	0.2
PMT quantum efficiency	0.3
PMT spreading factor	0.1
PMT average gain factor	10,000
Load resistance R_L	5 MΩ
Operating temperature	300 K
Rayleigh scattering coefficient k_s^{ray}	0.338/km
Mie scattering coefficient k_s^{mie}	0.421/km
Absorption coefficient k_a	1.202/km

The bit rate is set to be 1 Mbps and the T_x/R_x angle pair is set to be (10°, 10°). Theoretical calculation results and Monte-Carlo simulation results are shown in Fig. 2. A good agreement between the theoretical curves and the simulation curves is achieved, and the simulation results verify the correctness of the theoretical calculation.

If weak turbulence is assumed, with $C_n^2 = 10^{-17}$, the BER curve is almost the same as the counterpart of no turbulence. As the strength of the turbulence increases, the BER performance deteriorates obviously, especially at short baseline distances. For medium turbulence, with $C_n^2 = 5 \times 10^{-16}$, the BER performance deterioration is about 1 order of magnitude at the distance of 500 m. For strong turbulence, with $C_n^2 = 5 \times 10^{-15}$, the performance deterioration is about 5 orders of magnitude

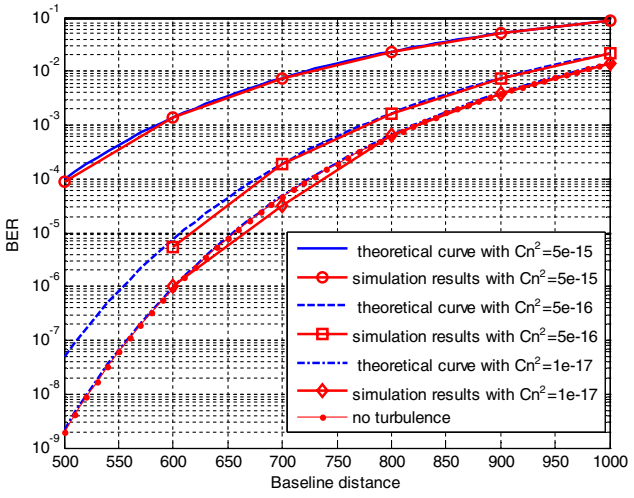

Fig. 2. BER versus baseline distance under different strengths of atmospheric turbulence.

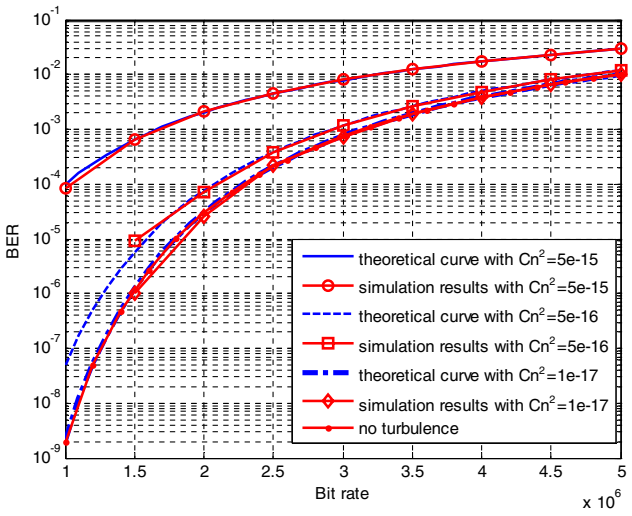

Fig. 3. BER versus bit rate under different strengths of atmospheric turbulence.

of that at the same distance. At a given BER level (10^{-3}), the communication distance can reach 830 m under no turbulence; under medium turbulence conditions ($C_n^2 = 5 \times 10^{-16}$) the communication distance is reduced to 770 m. While under strong turbulence conditions ($C_n^2 = 5 \times 10^{-15}$), the communication distance is only 580 m, and the communication distance is shortened by 30%.

The baseline distance is set to be 500 m, and the T_x/R_x angle pair is set to be (10°, 10°). Theoretical calculation results and simulation results are shown in Fig. 3. A good agreement between the theoretical curve and the simulation curve is achieved; simulation results verify the correctness of theoretical calculations.

Under the weak turbulence condition ($C_n^2 = 10^{-17}$), the impact of turbulence on BERs can be ignored. As C_n^2 increases to 5×10^{-16} and 5×10^{-15}, the BER curves become more and more flat, and the BERs become more and more insensitive to the variation of bit rate.

At a given BER level (10^{-3}), the bit rate reduces from 3.2 Mbps (no turbulence) to 1.6 Mbps ($C_n^2 = 5 \times 10^{-15}$) and the communication rate is reduced by half under strong turbulence conditions. The simulation results also reveal that if a low BER level (below 10^{-5}) is requested, under no turbulence, a bit rate above 1.5 Mbps could be achieved to satisfy video communication, while under strong turbulence conditions ($C_n^2 = 5 \times 10^{-15}$), the communication rate is reduced to hundreds of Kbps (from the tendency of the curve), only to satisfy audio communication.

The BERs under different T_x/R_x angle pairs is numerically evaluated in this section. The baseline distance is set to be 500 m, and the bit rate is set to be 1 Mbps. The numerical results under no turbulence, weak, medium, and strong turbulence conditions are shown in Figs. 4(a)–4(d), respectively.

As Fig. 4(b) illustrates, with $C_n^2 = 10^{-17}$, the impact of weak turbulence is negligible. As the strength of turbulence increases, with C_n^2 changes to 5×10^{-16} and 5×10^{-15}, there will be a noticeable degradation of the BER performance, particularly at small T_x/R_x angle pair and the BERs will become insensitive to the variation of the T_x/R_x angle pair.

If a BER level (below 10^{-3}) is requested, at a given T_x angle of 10°, under no turbulence, the R_x angle can change from 0° to 30° to meet this requirement; under medium turbulence, the R_x angle can change from 0° to 20°, while

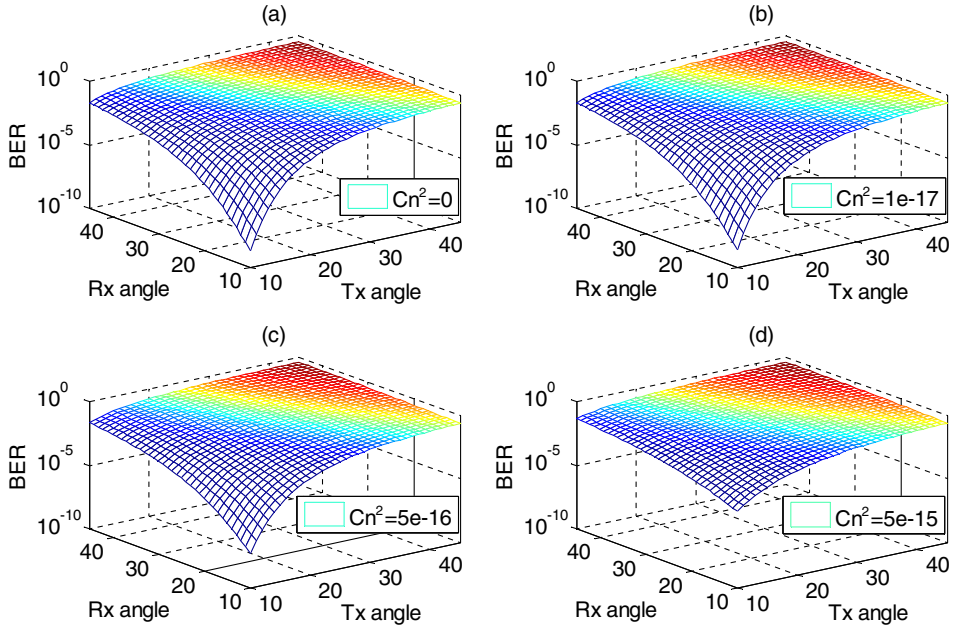

Fig. 4. BER versus T_x/R_x angle; (a) no turbulence, (b) under weak turbulence, (c) under medium turbulence, and (d) under strong turbulence.

under strong turbulence, the R_x angle can only change from 0° to 17°.

In conclusion, the impact of atmospheric turbulence on the performance of NLOS UV communication is studied. The performance degradation under different strengths of turbulence is evaluated. The correctness of our calculation is verified by Monte-Carlo simulation. Under the no turbulence condition, when the T_x/R_x angle pair is (10°, 10°) and the bit rate is 1 Mbps, the communication distance can reach 830 m at the 10^{-3} BER level, while under the strong turbulence condition ($C_n^2 = 5 \times 10^{-15}$), the distance is shortened to 580 m. Under no turbulence, when the T_x/R_x angle pair is (10°, 10°) and the distance is 500 m, the bit rate can reach 3.2 Mbps at the 10^{-3} BER level; under strong turbulence conditions, the bit rate reduces by half. If a lower BER (10^{-5}) is requested, the communication rate can only achieve several hundreds of Kbps, and no longer satisfies the demands of video communication. In the end, when the distance is 500 m and the bit rate is 1 Mbps, for a 10° T_x angle under no turbulence, the R_x angle can range from 0° to 30° to satisfy the below 10^{-3} BER requirement, while under the strong turbulence condition, the R_x angle can only range from 0° to 17°.

This work was supported by the National Basic Research Program of China (Grant No. 2013CB329203), and the National High Technology Research and Development Program of China (Grant No. 2013AA013601).

References

1. J. M. Kahn and J. R. Barry, Proc. IEEE **85**, 265 (1997).
2. Z. Xu and B. M. Sadler, IEEE Commun. Magazine **46**, 67 (2008).
3. H. Dong, H. Zhang, K. Lang, B. Yu, and M. Yao, Chin. Opt. Lett. **12**, 052301 (2014).
4. R. M. Gagliardi and S. Karp, *Optical Communications*, 2nd ed. (Wiley, 1995).
5. C. Liu, Y. Yao, J. Tian, Y. Zhao, and B. Yu, Chin. Opt. Lett. **12**, S10101 (2014).
6. D. M. Reilly, "Atmospheric optical communications in the middle ultraviolet," M.S. Thesis (MIT, 1976).
7. Y. Zuo, H. Xiao, J. Wu, Y. Li, and J. Lin, Opt. Express **20**, 10359 (2012).
8. Y. Zuo, H. Xiao, J. Wu, Y. Li, and J. Lin, Opt. Lett. **38**, 2116 (2013).
9. M. Zhang, P. Luo, X. Guo, X. Zhang, D. Han, and Q. Li, Chin. Opt. Lett. **12**, 100602 (2014).
10. G. Chen, F. Abou-Galala, Z. Xu, and B. M. Sadler, Opt. Express **16**, 15059 (2008).
11. G. Chen, Z. Xu, H. Ding, and B. M. Sadler, Opt. Express **17**, 3929 (2009).
12. Q. He, Z. Xu, and B. M. Sadler, Opt. Express **18**, 12226 (2010).
13. A. S. Zachor, Appl. Opt. **17**, 1911 (1978).
14. M. R. Luettgen, J. H. Shapiro, and D. M. Reilly, J. Opt. Soc. Am. A **8**, 1964 (1991).
15. Z. Xu, H. Ding, B. M. Sadler, and G. Chen, Opt. Lett. **33**, 1860 (2008).
16. Y. Zuo, H. Xiao, J. Wu, Y. Li, and J. Lin, J. China Commun. **10**, 52 (2013).
17. W. K. Pratt, *Laser Communication Systems*, 1st ed. (Wiley, 1969).
18. G. R. Osche, *Optical Detection Theory for Laser Applications* (Wiley, 2002).
19. H. Ding, G. Chen, A. K. Majumdar, B. M. Sadler, and Z. Xu, Proc. SPIE **8038**, 80380J (2011).
20. K. Kiasaleh, IEEE Trans. Commun. **53**, 1455 (2005).
21. S. Karp and R. Gagliardi, IEEE Trans. Commun. Technol. **17**, 670 (1969).